Fault Detection for Automotive Shock Absorber

Journal of Physics: Conference Series **659** (2015) 012037 doi:10.1088/1742-6596/659/1/012037

Fault Detection for Automotive Shock Absorber

Diana Hernandez-Alcantara, Ruben Morales-Menendez

Tecnológico de Monterrey, School of Engineering and Sciences
Av Eugenio Garza Sada # 2501, Col. Tecnológico
64,849 Monterrey, Nuevo León, México

E-mail: { A00469139, rmm }@itesm.mx

Luis Amezquita-Brooks

Universidad Autonoma de Nuevo León
Av. Universidad S/N
66,451 San Nicolas de los Garza, Nuevo León, México

E-mail: amezquita-brooks@ieee.org

Abstract. Fault detection for automotive semi-active shock absorbers is a challenge due to the non-linear dynamics and the strong influence of the disturbances such as the road profile. First obstacle for this task, is the modeling of the fault, which has been shown to be of multiplicative nature. Many of the most widespread fault detection schemes consider additive faults. Two model-based fault algorithms for semi-active shock absorber are compared: an observer-based approach and a parameter identification approach. The performance of these schemes is validated and compared using a commercial vehicle model that was experimentally validated. Early results shows that a parameter identification approach is more accurate, whereas an observer-based approach is less sensible to parametric uncertainty.

1. Motivation

Safety processes and technologies typically improve the overall equipment effectiveness and plant efficiency, with benefits that drop to the bottom line. One study also showed the following benefits from embedded safety systems: 5% productivity increase, 3% reduction in production expenses, 5% reduction in maintenance costs, 1% savings in capital expenses and 20% reduction in insurance costs, [4]. Considering that an automobile is integrated by many systems, such as, transmission, steering, exhaust, cooling, electrical, gasoline engine, fuel supply, electrical, braking and suspension system; where each system is a set of interdependent parts fulfilling a specific function and capable of functioning on its own. These systems can fail due to any number of possible failures that may occur in the sensors, actuators and devices that integrate them.

Although the automobile is not a safety-critical system, several driving conditions can lead to lose the vehicle stability with fatal consequences. The World Health Organization [19] estimates that 2.2 % of the global mortality (around 1.24 million deaths) is related to vehicle collisions caused by multiple factors, e.g. human factors, road quality, vehicle design and its maintenance, etc. The economic cost of motor vehicle collisions is estimated at over US $ 100 billion per year in middle-income countries (i.e. 1 - 2 % of their gross national product). Therefore, the preservation of the safety and comfort of passengers are the most fundamental goals for vehicle manufacturers and automotive control engineers. This research will focus on the controlled shock absorbers of the *Semi-Active* (*SA*) suspension system.

The primary functions of an automotive suspension system are to [9]: (1) isolate the chassis motion from road irregularities, (2) keep the tire-road contact with minimal load variations, (3) resist roll of the chassis, (4) react to the control forces (longitudinal and lateral) produced by the tires and braking and driving torques, and (5) maintain the wheels in the proper steer and camber attitudes to the road. The last two objectives are related to the kinematic behavior of the suspension geometry which can be solid axle or independent suspension; while, the first three objectives directly depend on the vertical force that it must transmit from the tires to the chassis.

According to the capability to adjust the damping force, the automobile suspensions can be classified as: *passive*, *active* or *SA*. *Passive* suspensions are only able to dissipate the energy and their damping characteristics are time invariant, while active ones are able to store, dissipate and generate energy through a variable damping coefficient but they are very expensive to apply because require an external power supply. *SA* suspensions represent a good solution to control the vertical vehicle dynamics using lower energy consumption and lower cost.

A suspension is integrated by 3 main elements: (1) an elastic element (i.e. a coil spring) which delivers a force proportional and opposite to the suspension elongation, this part carries all the static load; (2) a damping element (i.e. shock absorber), which provides a dissipative force proportional and opposite to the elongation speed; this part delivers a negligible force at steady-state, but plays a crucial role in the dynamic behavior of the suspension and (3) a set of mechanical elements which links the suspended (sprung) body to the unsprung mass. From the dynamic point of view, the spring and the damper are the two key elements, [21].

A *SA* suspension has an adaptable shock absorber where the continuous variable damping coefficient adjusted by external control signals along a road surface offers much better comfort and road holding performance with respect to *Passive* suspensions. The most fundamental advantage is its cost-benefit in comparison with *Active* suspensions. Although, the variable absorbing force may only affect transient behavior of the suspension deflection and does not affect its steady state as in an *Active* damper, *SA* shock absorbers are efficient to manage the balance between comfort and road holding. During past decades, different *SA* damper technologies have been examined, whose bandwidth oscillates from 0 to 30 Hz. There are four main technologies of *SA* shock absorbers in the market: *Electro-Hydraulic*, *Pneumatic*, *Magneto-Rheological* (*MR*), and *Electro-Rheological*.

An extensive work on *SA* suspension control systems emphasizes that *Magneto-Rheological* shock absorbers are one of the best solutions to manage the compromise between comfort and road holding. The transient response time of *MR* shock absorbers is around 12 ms, the power requirement is lower, they are robust to extreme temperature variations, and they are easier to manufacture and implement [5]. However, the use of these *MR* shock absorbers increases the necessity of fault detection. It has been noted that *SA* shock absorbers are more susceptible to faults. This is specially relevant since the effect of damper faults could vary from the increase of chassis vibrations to the loss of stability.

This paper, an extended version of [12], is organized as follows: Section 2 briefly reviews previous works on Fault Detection and Isolation for *SA* suspensions Section 3 defines the vehicle model. Section 4 describes the proposal. Section 5 discusses the results. Section 6 concludes the research project.

2. State of the art

Failures are inevitable and unpredictable in vehicle suspensions. The considered fault as case of study is represented as a loss of oil in an automobile shock absorber. There are different aspects that cause a damper leakage [20], which are related to a bad installation, an excessive use, a damage by external devices or a bad design of control system that saturates the manipulation. The direct consequence of a faulty shock absorber is the loss of damping force that causes a performance reduction in the suspension capabilities (comfort and safety for passengers) at any driving situation.

There are few papers dealing with *Fault Detection and Isolation* (*FDI*) for *SA* shock absorbers, and most of them are based on methods that inherently handle additive faults. These methods have the advantage of low computational requirements and do not need permanent excitation.

FDI modules based on analytical redundancy are the most accepted strategies for fault diagnosis and estimation [28]; especially parity-space approaches, because of its applicability to nonlinear systems, speed of detection, isolability property, robustness and computational complexity. Some FDI approaches, based on parity space theory, have been proposed for automotive suspensions [8], [16] to diagnose faults in actuators or sensors. However, these approaches have been designed for *Linear Time Invariant* (*LTI*) systems without consideration of model uncertainties or noisy measurements.

[18] explored an optimized parity space approach for actuator *FDI*. The parity spaces spans all the parity relations that quantify the analytical redundancies available between the sensor outputs and the actuator inputs. A transformation matrix is then optimized to transform these parity relations into residuals that are especially sensitive to specific actuator faults. Actuator faults cause the variance of parity space residuals to increase. A *CUmulative SUMmation* (*CUSUM*) procedure is used to determine when residual variance has changed sufficiently to indicate an actuator fault. The added advantage of this design procedure is that it uses less computational power than some other *FDI* systems such as a bank of extended *Kalman* filters.

In [24] the parity space method is used to detect the damper fault. However, the *SA* damper nonlinearities are not considered nor model uncertainties. An extension of the *FDI* module based on parity space theory by adding robustness to exogenous unknown disturbances is proposed by [23]. A novel Fault-Tolerant Controller is proposed for an automotive suspension system based on a*Quarter of Vehicle QoV* model. The design is divided in a robust *Linear Parameter Varying* (*LPV*) controller used to isolate vibrations from external disturbances and in a compensation mechanism used to accommodate actuator faults. The compensation mechanism is based on a robust fault detection and estimation scheme that reconstructs a fault on the *SA* damper; this information is used to reduce the failure effect into the vertical dynamics to achieve good control performances. Results show the effectiveness of the fault-tolerant *SA* damper versus an uncontrolled damper.

[1, 2] presented a fault detection method for suspension system using continuous wavelet transform in which Morlet wave function is used to determine the natural frequencies and amplitudes of signal components and include maximum contribution to the signal energy at the specific scale. Fault diagnosis has been investigated for dampers and upper damper bushings. After determination of faulty parts of suspension system by using signal energy distribution, by observing the changes in the natural frequencies and corresponding energy amplitudes, damper fault is distinguished from damper bushing fault.

[27] presents an application of a diagnosis and a fault tolerant control method for an active suspension system. The method detects and identifies an actuator fault and reconfigures the controller to maintain the ride comfort and vehicle performance in the presence of road disturbances. The proposed scheme consists of a diagnosis module and a controller reconfiguration module. The diagnosis module is based on the *Unknown Input Observer* (*UIO*)approach to detect and identify actuator faults. A bank of observers is designed to generate residual signals such that each of them matches the system in a defined actuator fault mode. The controller reconfiguration module consists of a bank of controllers, each corresponding to a fault mode of the system. The module changes the control law after the detection and the identification of an actuator fault. In [25] a Lyapunov based restoring force observer that leads to the design of a robust fault detection system is proposed. The fault estimation method provides a direct estimate of fault (i.e. stiffness and damping variations).

[29] designed a fault detection filter in finite frequency domain. A sufficient condition for residual system with the prescribed H_∞ performance index is derived based on the generalized *Kalman-Yakubovich-Popov* lemma. The fault detection filter is designed in middle-frequency domain such that the residual systems are asymptotically stable. Results are validated with a numerical example.

Even more focus on control, [6] demonstrated the efficiency of the *LPV* framework for vehicle dynamics control, when some actuators may be in failure (e.g. suspension and braking actuators failures). A LPV/H_∞ fault tolerant gain-scheduled vehicle dynamic control involving the steering actuators, rear brakes and four suspension systems is proposed for yaw stability, lateral and vertical

vehicle performances. The *LPV* control system can handle such failures through online adaptation of the control input distribution. Simulation results on a model experimentally validated (e.g. Renault Mégane Coupé) show the proposed methodology is effective and robust. Based on same LPV/H_∞ framework, [17] introduced a new *Fault Tolerant Control* (*FTC*) for a faulty semi-active suspension system (e.g. oil leakages damper). A fast adaptive fault algorithm is used to estimate the fault. Then, the *LPV-FTC* is designed to ensure the damper dissipativity constraint and to achieve the designed performance objectives in both comfort and road holding. The controller solution is based on the *LMI* solution for polytopic systems

Some *FDI* approaches based on parametric identification have been also proposed. These approaches have the advantage of providing deeper insight into the process; however, most online estimation methods need excitation and other operating requirements which may be restrictive when the road profile is unknown. [26] presented two simple models for the vertical dynamics. A two-step scheme for fault diagnosis is proposed, which consists of a detection of the fault in the first step and a fault diagnosis in the second. Results with measured data, drawn from a test rig showed that fault detection with parameter estimation leads to good results. Several different faults can be distinguished due to their unique patterns of the estimated parameter changes. Also, parity equations enable detection of some faults and require only little computational effort. Weak dampers can be detected.

Artificial Intelligence approaches had been exploited too. For automatic fault detection, estimated parameters were mapped to the different faults, [3]. Neuronal networks (e.g. feedforward perceptron networks) were proven for such tasks, the generalization error was below 4 %. Even a *FDI* system was implemented with parameter estimation, the process has to be excited all the time to guarantee convergence of the estimation algorithm. Then, parity equations were combined because they do not need permanent excitation and require less computational effort. Also, [7] designed the *FDI* system by developing the parity equations based on simple kinematical equations and on models of the lateral vehicle dynamics. The calculated residuals are then used for fuzzy logic fault diagnosis. The detection and diagnosis of sensor and process faults, as well as sensor reconfiguration, were presented for lateral and vertical vehicle dynamics. Small faults could be detected with a good isolation performance.

Two different approaches are applied to *SA* shock absorbers to estimate faults: the observer-based approach and the parameter estimation approach. The advantages and disadvantages of each method are analysed in order to determine which one is more suitable to estimate actuator faults in a *SA* suspension systems.

3. Quarter of Vehicle model

A *QoV* model is the most basic automotive suspension, Fig. 1. Its use assumes an equivalent load distribution among the four corners and a linear dependency with respect to the translational and rotational chassis motions. The lateral and longitudinal wheel dynamics is not considered, while the wheel road contact is ensured.

This very simple one-dimensional model consists of a spring-damper-system representing the suspension strut and a single spring replacing the tire. This friction element is added to estimate offset values to detect offset faults, or increased friction. The damper contributes the drive safety and the drive quality to the same extent. Its tasks are the prevention of an amplification of the body and the prevention of a skipping wheel. A non-skipping wheel is the condition for a good road-contact. The task of the spring is to carry the body-mass and to isolate the body from road disturbances maximally. A *QoV* model is a well-known simplification for vertical dynamics analysis of vehicle, [3]. Faults occurring in the damping system can be as a result of one or more of the following factors (numbered in Fig. 1): (1) Damage of leak of the damper, (2) Weak springs, (3) Worn bushing and broken of support member assembly, (4) the looseness joins, (5) under-inflation or over-inflation of tyres and (6) wear of the tyre.

The dynamic behavior of a *QoV* model with a *SA* suspension is described by:

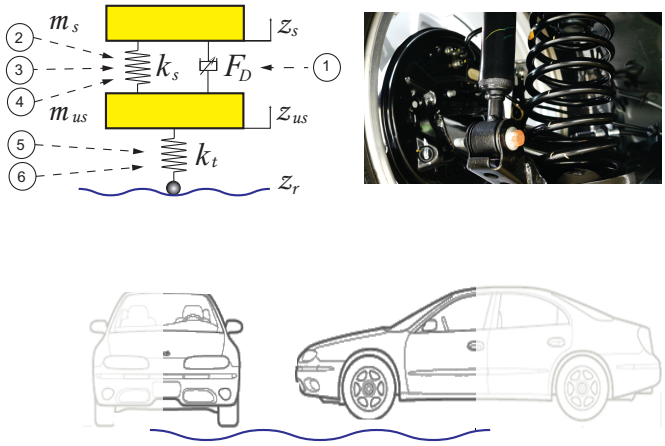

Figure 1. *QoV* model

$$\begin{aligned} m_s\ddot{z}_s &= -F_D - k_s(z_s - z_{us}) \\ m_{us}\ddot{z}_{us} &= k_s(z_s - z_{us}) + F_D - k_t(z_{us} - z_r) \end{aligned} \tag{1}$$

where z_s, z_{us} and z_r are the sprung mass, unsprung mass and road profile vertical positions, respectively; m_s is the sprung mass which represents the chassis, m_{us} is the unsprung mass which represents the wheel, tire, etc.; k_s and k_t are the suspension and the tire stiffness, and F_D represents the damping force.

The *SA* damper force behavior may be represented according to, [10]:

$$F_{SA} = k_p z_{def} + c_p \dot{z}_{def} + f_c \upsilon \tanh(a_v \dot{z}_{def} + a_d z_{def}) \tag{2}$$

where $z_{def} = z_s - z_{us}$ is the suspension deflection, and υ is the damper control input (*i.e* electric current for a *MR* damper), f_c is the force due to the input, c_p is the viscous damping coefficient, k_p is the stiffness coefficient, a_v and a_d are coefficients which characterize the hysteretic behavior, Table 1.

The considered model for multiplicative fault is :

$$F_D = \alpha[k_p z_{def} + c_p \dot{z}_{def} + f_c \upsilon \tanh\left(a_v \dot{z}_{def} + a_d z_{def}\right)] \tag{3}$$

where α represents the effectiveness of the damper, *i.e.* $\alpha = 1$ is a healthy damper, $\alpha = 0$ represents a 100 % damper failure. The aim is to estimate α using the masses accelerations and the suspension deflection, while the road profile z_r is an unknown perturbation input, because it is expensive to measure.

4. Approaches

Two complementary model-based fault estimation schemes for *SA* shock absorbers are proposed: an observer-based approach, which is intended to estimate additive faults; and a parameter identification approach, which is intended to estimate multiplicative faults.

4.1. Observer-based Fault Estimation

A *FDI* system based on an *UIO* and the *QoV* model (1) is proposed. The idea is to synthesize a residual, which is sensitive to the damper fault and insensitive to disturbances (i.e. road profile). The damper fault is first modelled as an additive fault:

$$F_D = \bar{F}_D - F_\delta \tag{4}$$

where $\bar{F}_D$ is the nominal force (*i.e.* the force of a healthy damper) and F_δ is the loss of force due to the fault. By using (1), (3) and (4), a state space system is:

$$\begin{aligned} \dot{x}(t) &= Ax(t)+B_u u(t)+B_z z_r(t)+B_F F_\delta(t) \\ y(t) &= Cx(t)+D_u u(t)+D_z z_r(t)+D_f F_\delta(t) \end{aligned} \tag{5}$$

with

$$x=\begin{bmatrix} z_s & \dot{z}_s & z_{us} & \dot{z}_{us} \end{bmatrix}^\top, y=\begin{bmatrix} \ddot{z}_{us} & \ddot{z}_s & z_{def} \end{bmatrix}^\top$$

$$A=\begin{bmatrix} 0 & 1 & 0 & 0 \\ -\frac{k}{m_s} & -\frac{c_p}{m_s} & \frac{k}{m_s} & \frac{c_p}{m_s} \\ 0 & 0 & 0 & 1 \\ \frac{k}{m_{us}} & \frac{c_p}{m_{us}} & -\frac{k+k_t}{m_{us}} & -\frac{c_p}{m_{us}} \end{bmatrix} B_u=\begin{bmatrix} 0 \\ -\frac{f_c}{m_s} \\ 0 \\ \frac{f_c}{m_{us}} \end{bmatrix} B_z=\begin{bmatrix} 0 \\ 0 \\ 0 \\ \frac{k_t}{m_{us}} \end{bmatrix} B_F=\begin{bmatrix} 0 \\ -\frac{1}{m_s} \\ 0 \\ \frac{1}{m_{us}} \end{bmatrix}$$

$$C=\begin{bmatrix} \frac{k}{m_{us}} & \frac{c_p}{m_{us}} & -\frac{k+k_t}{m_{us}} & -\frac{c_p}{m_{us}} \\ -\frac{k}{m_s} & -\frac{c_p}{m_s} & \frac{k}{m_s} & \\ 1 & 0 & -1 & 0 \end{bmatrix} D_u=\begin{bmatrix} \frac{f_c}{m_{us}} \\ \frac{-f_c}{m_s} \\ 0 \end{bmatrix} D_z=\begin{bmatrix} \frac{k_t}{m_{us}} \\ 0 \\ 0 \end{bmatrix} D_f=\begin{bmatrix} \frac{1}{m_{us}} \\ \frac{-1}{m_s} \\ 0 \end{bmatrix}$$

where $k=k_s+k_p$, $u(t)=\upsilon\rho(t)$ and $\rho(t)$ is the nonlinear term of the *SA* damper model:

$$\rho(t)=\tanh\left(a_v\dot{z}_{def}+a_d z_{def}\right) \tag{6}$$

Note that system (5) is comprised by a linear subsystem in a closed loop with a memoryless nonlinear function $\upsilon\rho(t)$.

An important result of applying the *UIO* theory to this domain is, without road information, the system is non-observable and non-detectable [11]. This will affect the state estimations.

An approximated *UIO* observer can be obtained by decoupling the system (5) from the road surface using the procedure reported in [14]. The decoupled system can be written as:

$$\begin{aligned} \dot{x}(t) &= \bar{A}x(t)+\bar{B}_u\rho(t)u(t)+\bar{B}_F F_\delta(t)+Gy_1(t) \\ y_2(t) &= \bar{C}x(t)+\bar{D}_u\rho(t)u(t)+\bar{D}_f F_\delta(t) \end{aligned} \tag{7}$$

where

$$\bar{A}=\begin{bmatrix} 0 & 1 & 0 & 0 \\ -\frac{k}{m_s} & -\frac{c_p}{m_s} & \frac{k}{m_s} & \frac{c_p}{m_s} \\ 0 & 0 & 0 & 1 \\ 0 & 0 & 0 & 0 \end{bmatrix} \bar{B}_u=\begin{bmatrix} 0 \\ -\frac{f_c}{m_s} \\ 0 \\ 0 \end{bmatrix} \bar{B}_f=\begin{bmatrix} 0 \\ -\frac{1}{m_s} \\ 0 \\ 0 \end{bmatrix} G=\begin{bmatrix} 0 \\ 0 \\ 0 \\ 1 \end{bmatrix} \bar{C}=\begin{bmatrix} \bar{C}_1 \\ \bar{C}_2 \end{bmatrix}=\begin{bmatrix} 1 & 0 & -1 & 0 \\ -\frac{k}{m_s} & -\frac{c_p}{m_s} & \frac{k}{m_s} & \frac{c_p}{m_s} \end{bmatrix}$$

$$\bar{D}_u=\begin{bmatrix} \bar{D}_{u_1} \\ \bar{D}_{u_2} \end{bmatrix}=\begin{bmatrix} 0 \\ \frac{-f_c}{m_s} \end{bmatrix} \bar{D}_f=\begin{bmatrix} \bar{D}_{f_1} \\ \bar{D}_{f_2} \end{bmatrix}=\begin{bmatrix} 0 \\ \frac{-1}{m_s} \end{bmatrix},\ y_1=\ddot{z}_{us},\ y_2=z_{def},\ y_3=\ddot{z}_s,\ \bar{y}=\begin{bmatrix} y_2 \\ y_3 \end{bmatrix}$$

For the state estimation the decoupled system (7) with the output y_2 will be used since this output does not depend on the fault. For the residual generation, y_3, which is affected by the fault, will be used.

If $(\bar{A},\bar{C}_1)$ are observable or detectable, an observer can be designed for the decoupled system to estimate the states. The observability matrix of system (7), has rank 2; thus, two of the observer poles cannot be located arbitrarily. For the system (7) the non-observable subset is related to two poles in $s=0$; therefore, the system is non-observable and non-detectable. A possible solution consists on generating a stable system which approximates the frequency response of the *UIO* observer, [13].

An observer is a dynamical system whose inputs are the process input and output vectors. For the decoupled system (7), the observer poles in $s=0$ are related to the input contribution to the state estimation. Since these poles are not stable regardless the observer gain, the best estimation effort is the open-loop simulation of these states. In general the state estimation based only in the simulation of the process (which is equivalent to an observer with observer gain equal to zero) is not advised. However, the input related with these integrators is the unsprung-mass acceleration, which is indeed a measured output, but it was considered as an input to achieve the decoupling of the system from the road profile. Thus, the non-observable states are estimated via the output, like it is done by using high-gain observers.

The observer gain matrix L is designed to place the two observable poles at $(-20.38 \pm 1.09i)$. The resulting observer combines the closed-loop estimation dynamics and the integration of acceleration measurements. For the states, which are estimated by numerical integration, it is well known that low frequency noise in the measurements induces a divergence called drift [22]. Without additional measurements, it is not possible to eliminate the drift by modifying the observer gain, [11, 15]. Since the suspension deflection is limited and the masses velocities converge to zero, it is possible to use high-pass filters to eliminate the drift. Then, the observer is complemented by adding a pair of high-pass filters $g_f(s) = s/(s+\omega_f)$ for each of the integrators. Only the non-detectable states are filtered, while the observable ones are estimated by a closed-loop observer. The cut-frequency ω_f of the filter is set at 0.14 Hz.

By using the estimated states with the *UIO* observer and the measurement of the sprung mass acceleration, the residual can be computed to detect a fault (loss of damping force):

$$r(t) = y_3 - \left[\bar{C}_2\hat{x}(t) + \bar{D}_{u_2}u(t)\right] = \bar{D}_{f_2}F_\delta(t) \tag{8}$$

then the magnitude of the fault can be estimated as $\hat{F}_\delta = [\bar{D}_{f_2}]^\dagger r(t)$ where † stands for the *Moore Penrose* pseudo inverse.

4.2. Parameter Estimation Approach

By considering the multiplicative model of the fault in (3), the system can be represented in state-space form as:

$$\begin{array}{rcl} \dot{x}(t) & = & A_n x(t) + g(x,u)\alpha + B_z z_r(t) \\ y(t) & = & C_n(\alpha)x(t) + h(x,u)\alpha + D_z z_r(t) \end{array} \tag{9}$$

with

$$A_n = \begin{bmatrix} 0 & 1 & 0 & 0 \\ -\frac{ks}{m_s} & 0 & \frac{ks}{m_s} & 0 \\ 0 & 0 & 0 & 1 \\ \frac{ks}{m_{us}} & 0 & -\frac{ks+k_t}{m_{us}} & 0 \end{bmatrix} \quad g(x,u) = \begin{bmatrix} 0 \\ -\frac{f_c\rho u + c_p(x_2-x_4)+k_p(x_1-x_3)}{m_s} \\ 0 \\ \frac{f_c\rho u + c_p(x_2-x_4)+k_p(x_1-x_3)}{m_{us}} \end{bmatrix}$$

$$C_n = \begin{bmatrix} \frac{ks}{m_{us}} & 0 & -\frac{ks+k_t}{m_{us}} & 0 \\ -\frac{ks}{m_s} & 0 & \frac{ks}{m_s} & 0 \\ 1 & 0 & -1 & 0 \end{bmatrix} \quad h(x,u) = \begin{bmatrix} \frac{f_c\rho u + c_p(x_2-x_4)+k_p(x_1-x_3)}{m_{us}} \\ -\frac{f_c\rho u + c_p(x_2-x_4)+k_p(x_1-x_3)}{m_s} \\ 0 \end{bmatrix}$$

Although the fault affects both the sprung and unsprung mass dynamics, for this estimator only the sprung mass dynamic will be considered since it is independent of the unmeasured road profile. Two measurements are used: $\ddot{z}_s$ and z_{def}. From (9), the discrete-time representation of the sprung mass dynamic can be written in the regression form as $\zeta = \psi^\top\theta$ where $\zeta = -k_s(z_{def}) - m_s(\ddot{z}_s)$, $\psi^\top = -\frac{f_c\rho u + c_p(\dot{z}_{def})+k_p(z_{def})}{m_s}$ and $\theta = \alpha$. The damper fault can be online estimated by using the *Recursive Least Squares* (*RLS*) with forgetting factor λ :

$$\begin{array}{rr} e(k) = \zeta - \psi^\top(k)\hat{\theta}(k-1) & \gamma(k) = \frac{P(k-1)\psi(k)}{\lambda + \psi^\top(k)P(k-1)\psi(k)} \\ P(k) = \frac{1}{\lambda}(I - \gamma(k)\psi^\top(k))P(k-1) & \hat{\theta}(k) = \hat{\theta}(k-1) + \gamma(k)e(k) \end{array} \tag{10}$$

where $\hat{\theta}$ is the estimation of θ. The measurement of $\dot{z}_{def}$ is not available, therefore an estimation is required to implement the parameter estimation. $\dot{z}_{def}$ may be estimated either by the numerical derivative approximation of z_{def} or by an state-observer. In this case, an approximation based on the bandwidth-limited derivative is used.

For a sufficiently high sampling rate, the discrete estimator will approximate the continuous time model parameters. For this system the simulations show that 500 Hz was a sufficiently high sampling rate to have a good approximation.

Table 1. Commercial vehicle model parameters

Parameter	Value	Units	Parameter	Value	Units
m_s	315	Kg	m_{us}	37.5	Kg
k_s	29,500	N/m	k_t	230,000	N/m
c_p	1,500	Ns/m	k_p	-10,239	N/m
a_v	7.89	s/m	a_d	-13.8	1/m
f_c	441	Ns/A			

5. Results

Data from a commercial vehicle was used, Table 1.

Six tests were used to assess the performance of the *FDI* proposals. These tests consider a) an *ISO* Type *D* at a vehicle speed of 30 Km/h, and b) a series of bumps as road profile signals, which represents a normal driving conditions. Table 2 summarizes the tests characteristics.

Table 2. Tests used to evaluate the *FDI* methods.

Test	Description		Objective analysis
	α	Current	
#1	$[0.5, 1]$	$u = 2\ A$	Estimation of abrupt fault at constant damper input.
#2	$[0.1, 1]$	$u = 2\ A$	Estimation of gradual fault at constant damper input.
#3	$[0.1, 1]$	$u \in [0.5, 3]\ A$	Estimation of gradual fault at varying damper input.
#4	$[0.5, 1]$	steps in z_r	Sensitivity to road disturbances.
#5	$[0.5, 1]$	$1.2\ m_s$	Robustness to uncertainty in m_s.
#6	$[0.2, 1]$	$0.8\ K_t$	Robustness to uncertainty in k_t.

Although both strategies are used to estimate faults of different nature (*i.e.* additive or multiplicative), a comparison can be made by calculating the equivalence between them. From (4) and (3) the relation between the multiplicative and the additive faults can be obtained as $F_\delta = F_D\left(\frac{1}{\alpha} - 1\right)$.

Figure 2 (left plot) shows the estimation of the loss of force F_δ in the Test #1. An abrupt damper fault is modelled as a step change in α; however, the equivalent additive fault also depends on F_D, therefore even if α is constant, F_δ is not. This figure shows the *Least Squares Estimator* (*LEE*) error converges to zero for a step change in α, while the *Observer-Based Estimator* (*OBE*) error does not.

Figure 2 (right plot) shows the multiplicative equivalent fault of the Test #1, this confirms the last discussion. The *LEE* is better posed for constant multiplicative faults than the *OBE*. Since real damper faults are more similar to multiplicative faults, only this type of faults will be discussed.

Figure 3 (left plot) shows that both approaches are able to estimate gradual variations for multiplicative faults, Test # 2. When the multiplicative fault α has a constant slope, neither of the estimator errors converge to zero. The *LEE* has a lower overall error. In Fig. 3 (right plot) the estimation of α is compared in the same fault conditions as in Test #2, but, in this case a varying damper input ($[1, 3]\ Amp$) is considered. This is an important observation because this characteristic, is essential for *SA* suspension systems. This figure also shows that the *LEE* has lower sensitivity to damper input variation than the *OBE*.

Test #4 is used to asses the sensitivity of the fault estimators to sudden road profile changes, which can represent road abnormalities such as potholes. The road decoupling of the *OBE* is not perfect since a perfect *UIO* was not possible to design due to observability issues. This is more evident when the road presents sudden changes, inducing a greater level of error. The *LEE* is not visibly affected by these road characteristics, Fig. 4 (left plot).

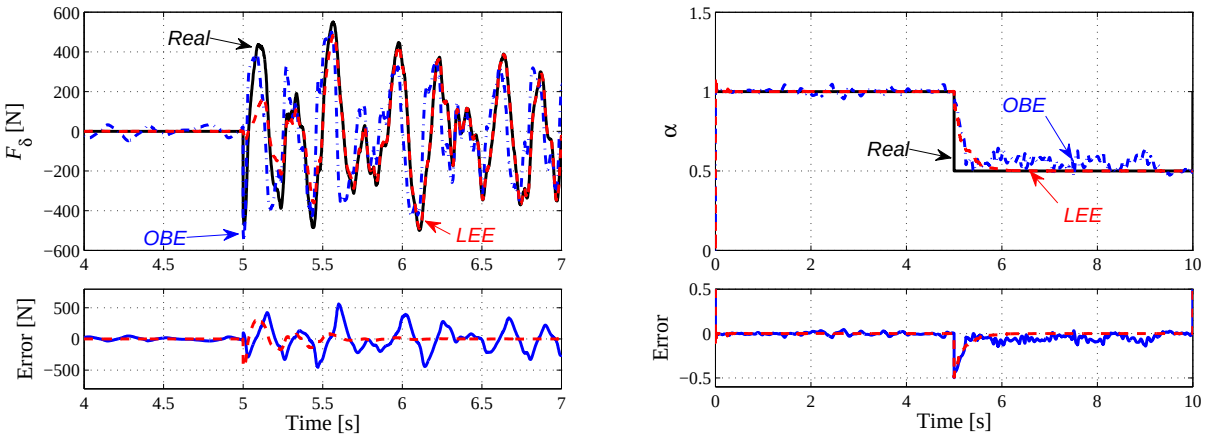

Figure 2. Comparison of estimated force loss and fault α in Test #1 (*ISO* Type *D*).

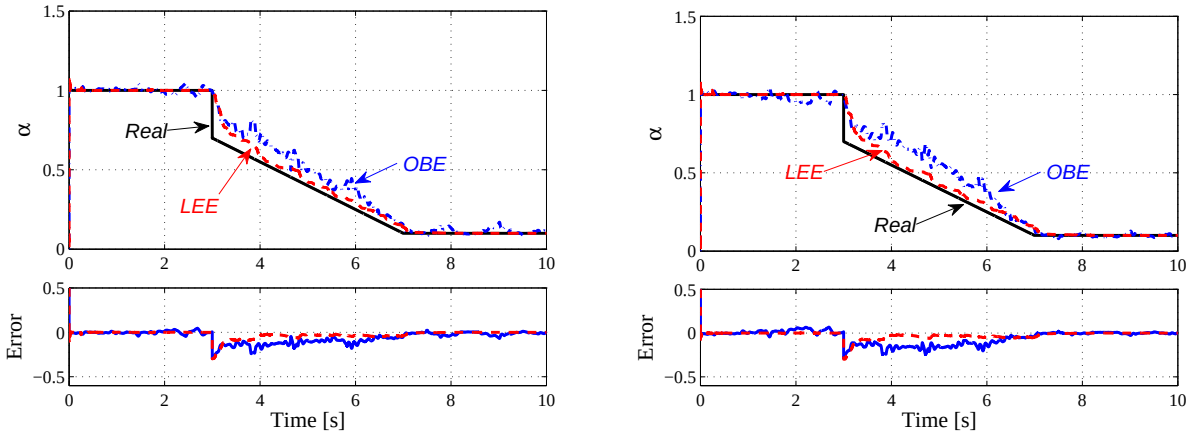

Figure 3. Comparison of estimated fault α in Tests #2 and #3 (*ISO* Type *D*).

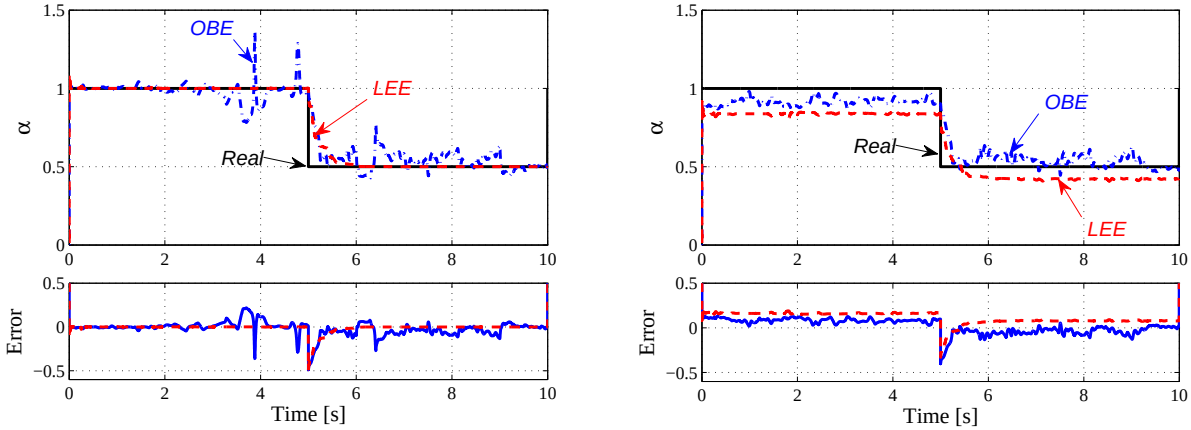

Figure 4. Comparison of estimated fault α in Tests #4 and #5 (*ISO* Type *D*).

Figure 4 (right plot) is used to assess the effect of sprung mass uncertainty on the estimated fault, a sprung mass 20% heavier was considered. The results show, that the mass uncertainty induces steady state error in both algorithms. The *LEE* has a greater error.

Figure 5 (left plot) shows the estimated fault in the Test #1 under other road condition, the series of bumps. As observed in this figure, the *LEE* is less sensitive to the road profile and it presents a lower error level. The *LEE* is better posed for constant multiplicative faults than the *OBE*. In Fig. 5 (right plot), it can be observed that he *LEE* has lower sensitivity to damper input variation than the *OBE*.

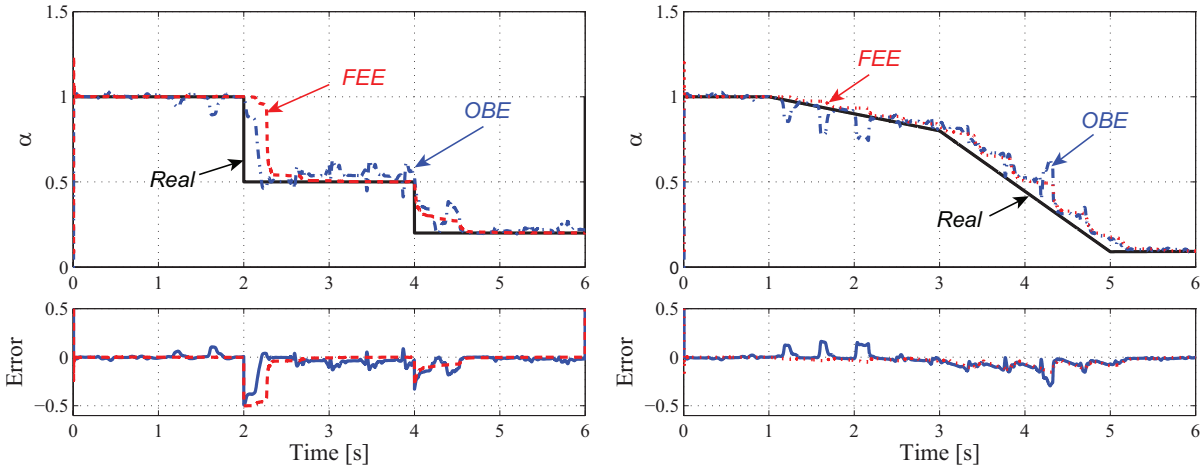

Figure 5. Comparison of estimated fault α in Test #1a and #3a (Series of bumps).

Test #6 is used to evaluate the effect of tire stiffness uncertainty on the estimated fault. This variation may occur due to variations in the tire inflation pressure. A 20% lower tire stiffness was considered, which corresponds to a variation of 5 psi in the inflation pressure. The results in Fig. 6 show that both methods are robust to the uncertainty in this parameter. The *OBE* error is slightly higher, 10 % with respect to the unperturbed case, whereas the estimation of the *LEE* is not affected since it is independent of this parameter.

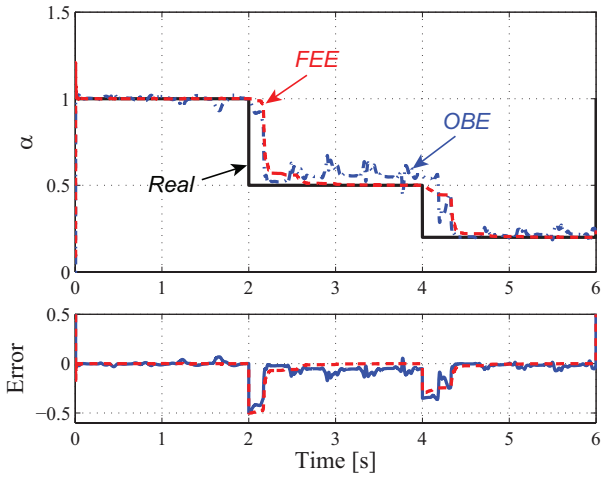

Figure 6. Comparison of estimated fault α in Test #6 (Series of bumps).

Finally, a quantitative comparison of the approaches was made using the *Root Mean Square Error*

(*RMSE*) index. Table 3 summarizes the results. It can be observed that the *LEE* presents an overall lower level of error; for instance, in Test #2 the *LEE* has 493% lower *RMSE* in the estimation of the loss of force F_δ. If the fault is represented in the multiplicative form, the *LEE* also yields a lower *RMSE*, but the differences are smaller. For example, in test #2 the *LEE* is also lower but 57%. Only when sprung-mass uncertainty is considered the *OBE* has a lower index, in this case 55% lower for F_δ.

Table 3. *RMSE* of fault estimation approaches under different scenarios.

Test	Road Profile	*OBE*		*LEE*	
		F_δ	α	F_δ	α
1	*ISO* Type *D*	1.46221	0.00062	0.36250	0.00050
2	*ISO* Type *D*	2.40880	0.00071	0.40596	0.00045
3	*ISO* Type *D*	1.78609	0.00080	0.41011	0.00044
4	*ISO* Type *D*	1.66067	0.00073	0.34299	0.00049
5	*ISO* Type *D*	1.51313	0.00077	0.91140	0.00120
1a	Series of bumps	1.74457	0.00106	0.97300	0.00121
3a	Series of bumps	1.75683	0.00077	1.16826	0.00065
6	Series of bumps	1.71662	0.00119	0.89106	0.00121

6. Conclusions

A comparison of two fault detection algorithms for the estimation of *semi-active* shock absorber faults is presented. One method is based on classical least square parametric identification to estimate a multiplicative fault. The second method is based on an *Unknown Input Observer*, which is used to calculate a residual and to estimate the loss of force due to an additive fault.

It has been reported that shock absorber faults are normally of multiplicative nature; nonetheless, additive fault estimation methods are more widely reported. Since it is possible to derive the multiplicative equivalent from the additive estimation, both methods were compared through different scenarios, including mass uncertainty, shock absorber input sensitivity and road profile sensitivity. The results show that the *Least Squares Estimator* achieves better qualitative and quantitative performance in all cases, with the exception of mass uncertainty. This also suggests that, for this system, identification algorithms based on regression models are highly sensible to process parameters changes. It can be concluded that the two estimators present complementary characteristics which could be exploited depending on the operating conditions to improve the overall system performance. The results also show that for this application a simple fault estimation algorithm, such as *Least Squares Estimator*, is enough as long as a multiplicative fault structure is used and a low level of parameter uncertainty is present.

Acknowledgment

Authors thank *Tecnológico de Monterrey* and *CONACyT* because the *Automotive Consortium* and bilateral PCP 06/13 (México-France) project.

References

[1] S. Azadi and A. Soltani. Application of Wavelet Analysis to the Suspension System Fault Detection of a Vehicle. In *SAE 2007 Noise and Vibration Conf. and Exhibition*, USA, 2007. Technical paper 2007-01-2370.

[2] S. Azadi and A. Soltani. Fault Detection for Passive Suspension Systems using Wavelet Transform. In *SAE 2007 Noise and Vibration Conf. and Exhibition*, USA, 2007. Technical paper 2007-01-2368.

[3] M. Börner, R. Isermann, and M. Schmitt. A Sensor and Process Fault Detection System for Vehicle Suspension Systems. In *SAE 2002 World Congress & Exhibition*, USA, 2002. Technical paper 2002-01-0135.

[4] ABB Consulting. 5 Ways to Improve Safety and Profitability, without Disrupting Operations. *White paper*, pages 1–5, 2015.
[5] J.C. Dixon. *The Shock Absorber Handbook*. Wiley Ed., 2^{nd} Ed., 2007.
[6] S. Fergani, O. Sename, L. Dugard, and P Gáspár. Further Development on the LPV Fault Tolerant Control for Vehicle Dynamics. In *Preprints of* 9^{th} *IFAC-Safeprocess*, pages 24–29, France, Sept 2015.
[7] D. Fischer, M. Börner, J. Schmitt, and R. Isermann. Fault Detection for Lateral and Vertical Vehicle Dynamics. *Control Eng. Practice*, 15:315–324, 2007.
[8] D. Fischer and R. Isermann. Mechatronic Semi-Active and Active Vehicle Suspensions. *Control Eng. Practice*, 12:1353–1367, 2004.
[9] T.D. Gillespie. *Fundamentals of Vehicle Dynamics*. Society of Automotive Engineers, Inc., 1992.
[10] S. Guo, S. Yang, and C. Pan. Dynamical Modeling of Magneto-Rheological Damper Behaviors. *J. of Intell. Mater., Syst. and Struct.*, 17:3–14, 2006.
[11] J.K. Hedrick, R. Rajamani, and K. Yi. Observer Design for Electronic Suspension Applications. *Vehicle Sys Dyn*, 23(1):413–440, 1994.
[12] D. Hernández-Alcantara, R. Morales-Menendez, and L. Amezquita-Brooks. Fault Estimation Methods for Semi-Active Suspension Systems. In *to appear in XVII Int. Autum Meeting on Power, Electronics and Computing*, México, Nov 2015.
[13] D. Hernández-Alcantara, J.C. Tudón-Martínez, L. Amezquita-Brooks, C. Vivas-Lopez, and R. Morales-Menendez. State Observers for Semi-Active Suspensions: Experimental Results. In *IEEE Multi-Conf on Systems and Control*, France, 2014.
[14] M. Hou and P.C. Muller. Design of Observers for Linear Systems with Unknown Inputs. *IEEE Trans Autom Control*, 37(6):871–875, 1992.
[15] Ling-Yuan Hsu and Tsung-Lin Chen. Vehicle Full-State Estimation and Prediction System Using State Observers. *IEEE Trans on Vehicular Tech*, 58(6):2651–2662, July 2009.
[16] H. Kim and H. Lee. Fault-Tolerant Control Algorithm for a Four-Corner Closed-Loop Air Suspension System. *IEEE Transactions on Industrial Electronics*, 58(10):4866–4879, 2011.
[17] M.Q. Nguyen, O. Sename, and L. Dugard. An LPV Fault Tolerant Control for Semi-Active Suspension - Scheduled by Fault Estimation. In *Preprints of* 9^{th} *IFAC-Safeprocess*, pages 42–47, France, Sept 2015.
[18] Hendrik M. Odendaal and Thomas Jones. Actuator Fault Detection and Isolation: An Optimised Parity Space Approach. *Control Eng Practice*, 26(0):222 – 232, 2014.
[19] World Health Organization. Global Status Report on Road Safety, 2013.
[20] Sachs. Shock Absorbers Leak, Potential Causes. Technical report, Sachs, www.zfsachs.com, 2008.
[21] S.M. Savaresi, C. Poussot-Vassal, C. Spelta, O. Sename, and L. Dugard. *Semi-Active Suspension Control for Vehicles*. Elsevier - Butterworth Heinemann, 2010.
[22] U-X Tan et al. Estimating Displacement of Periodic Motion with Inertial Sensors. *IEEE Sensors J*, 8(8):1385–1388, 2008.
[23] J.C. Tudón-Martínez, S. Varrier, R. Morales-Menendez, R. Ramírez-Mendoza, D. Koenig, J-J. Martínez, and O. Sename. Fault Tolerant Control with Additive Compensation for Faults in an Automotive Damper. In *Proc. of the* 10^{th} *IEEE Int Conf on Networking, Sensing and Control*, pages 810–814, France, 2013.
[24] S. Varrier, J.J. Lozoya-Santos, D. Hernandez, D. Koenig, J-J. Martínez, and R. Morales-Menendez. Fault Detection in Automotive Semi-active Suspensions: Experimental Results. In *Proc. of SAE World Congress 2013*, USA, 2013. Technical paper: 2013-01-1234.
[25] Y. Vidal, L. Acho, F. Pozo, and J. Rodellar. Fault Detection in Base-Isolation Systems via a Restoring Force Observer. In *Conf. on Control and Fault Tolerant Systems*, pages 777–782, France, 2010.
[26] T. Weispfenning. Fault Detection and Diagnosis of Components of the Vehicle Vertical Dynamics. *Meccanica*, 32(5):459–472, 1997.
[27] A. Yetendje, M. Seron, and J. De Dona. Diagnosis and Actuator Fault Tolerant Control in Vehicle Active Suspension. In *Int Conf on Information and Automation for Sustainability*, pages 153–158, Australia, 2007.
[28] Y. Zhang, J. Sheng, S. J. Qin, and T. Hesketh. Dynamic Process Monitoring using Multiscale PCA . In *IEEE Conf on Electrical and Computer Eng*, pages 1579–1584, May 1999.
[29] X. Zhu, Y. Xia, S. Chai, and P. Shi. A Finite-Frequency Domain Approach to Fault Detection Filter Design for Vehicle Active Suspension Systems. In *Proc of the* 11^{th} *World Congress on Intelligent Control and Automation*, pages 485–490, China, Jun 2014.